C. R. Geoscience 346 (2014) 317–325

Contents lists available at ScienceDirect

Comptes Rendus Geoscience

www.sciencedirect.com

Petrology, geochemistry

The Earth as a multiscale quantum-mechanical system

Pascal Richet [a,*], Giulio Ottonello [b]

[a] Institut de physique du globe de Paris, 1, rue Jussieu, 75005 Paris, France
[b] DISTAV, Universitâ di Genova, Corso Europa 26, 16132 Genova, Italy

ARTICLE INFO

Article history:
Received 30 June 2014
Accepted after revision 5 September 2014
Available online 13 November 2014

Keywords:
Magmatic differentiation
ab initio calculations
SiO_2 polymorphs
Silicon-oxygen bonding
Aluminum charge compensation
Noble gas solubility

ABSTRACT

Major features of the Earth's structure and dynamics originate in the contrast between the rigidity of Si–O bonds and the softness of Si–O–Si linkages. Because this contrast results from orbital hybridization, a real understanding of bonding relies on *ab initio* quantum-mechanical principles. As investigated with first-principles interatomic potentials, the α–β transitions of SiO_2 polymorphs illustrate how soft Si–O–Si linkages give rise to dynamical structures at rather low temperatures and yield the low melting temperatures of SiO_2-rich minerals that are at the roots of SiO_2 enrichment in magmatic differentiation. The increasing concentration of alkalis throughout this process is another aspect that must also be studied in terms of molecular orbitals in relation with the presence of aluminum in tetrahedral coordination. Finally, calculations of noble gas solubility show that some important features can be treated with "hybrid" calculations when, in addition to quantum-mechanical effects, the energy needed to create a cavity in the silicate melt is dealt with in a classical manner.

1. Introduction

Ever since the earliest phases of the history of our planet, the main physical and chemical features of the Earth have been determined by magma differentiation. Continent growth has for instance been the ultimate result of fractional crystallization whereby basaltic magma, formed by partial melting of mafic rocks at depth, progressively gives rise to rhyolitic or phonolitic melts through precipitation and settling of SiO_2-poor ferromagnesian minerals not far from the Earth's surface. Depending on the initial composition of magma, the petrogenetic series that have been distinguished are characterized by different evolutions (Fig. 1), but they share the common feature of marked relative increases in the contents of SiO_2, Al_2O_3 and, especially, of alkali oxides. Correlatively, strong decreases in the contents of alkaline earth oxides take place. These systematic changes in chemical composition induced by fractional crystallization are associated with important variations of physical properties, which have themselves far-reaching consequences for magma transfer and geodynamic processes. To give a single example, continents are less dense than the mantle so that they escape subduction cycles and remain distinct from the upper mantle simply because of the impossibility to pack compactly SiO_4 and AlO_4 tetrahedra in the three-dimensional networks of quartz and feldspars, the two main constituents of granite.

Curiously, however, the fundamental principles governing magma differentiation have received little attention, even though Osborn (1950) long ago pointed out the relevance of ion properties such as field strength and electronic configuration. Actually many basic features of silicates such as the four-fold coordination of Si^{4+} cations by oxygen anions can be accounted for in terms of ionic forces (cf. Mysen and Richet, 2005). But it is generally

* Corresponding author.
E-mail address: richet@ipgp.fr (P. Richet).

http://dx.doi.org/10.1016/j.crte.2014.09.003
1631-0713/

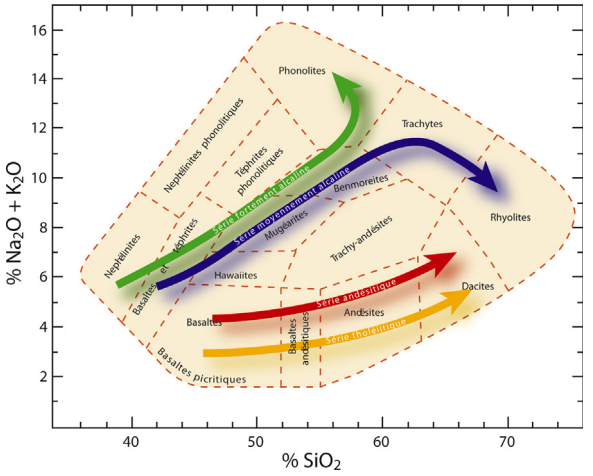

Fig. 1. (Color online.) The main petrogenetic series, beginning with the various types of basalt magma and ending with phonolites, rhyolites and dacites, as indicated by the variations of SiO_2 and alkali oxide contents. Cox et al., 1979.

incorrect to assume complete electron transfer between the oxygen and the metals with which they bond and, thus, to approximate anions and cations as closed shells interacting through Coulombic forces and short-range repulsion. In other words, fundamental issues in Earth sciences cannot be addressed in terms of atomic bonding with the assumption that bonding lacks directionality and depends only on nominal ionic charges and interatomic distances.

Hence, the question that remains to be investigated is how the structure and dynamics at all length scales within the Earth are determined at a microscopic scale by interatomic potentials and chemical bonds and, thus, by electronic distributions between bonded atoms. As stated in these terms, major questions of geochemical and geophysical interest can be answered only within the framework of quantum mechanics. Even though various kinds of first-principles calculations are now routinely performed not only for minerals, but also for melts (*e.g.*, Ispas et al., 2001), they have generally focused on specific problems in mineral physics without specifically addressing their broad geochemical or geophysical consequences.

In this paper, our goal is to substantiate our claim that, despite its immense size, the Earth as we know it has to be studied from a quantum-mechanical perspective. It would be far beyond our scope to review even briefly the quantum-mechanical methods currently used to investigate bonding in condensed phases (*e.g.*, Gatti, 2005). Rather we will discuss in general terms four different topics. We will first examine the α–β transitions of tectosilicates to show that the anomalously low melting temperature of SiO_2, which is at the very roots of magma differentiation, is a direct consequence of soft Si–O–Si linkages. We will then examine this directionality in terms of orbital hybridization in pure SiO_2 before turning to a closely related question, namely, the manner in which AlO_4 tetrahedra are stabilized within the silicate networks of SiO_4 tetrahedra thanks to electron transfer from charge-compensating cations. We will finally consider the supposedly inert noble gases, whose relative abundances carry important information on the Earth's early history (*e.g.*, Ozima and Pososek, 2001), to discuss how their solubility in silicate melts is determined by the creation of cavities large enough to host them. Basic quantum-mechanical concepts and common acronyms have to be used to deal with these issues. Rather than introducing them anew, we prefer to refer to Tossel and Vaughan (1992) for an introduction to the realm of "Quantum Geochemistry".

2. α–β transitions and melting of tectosilicates

The considerable SiO_2 enrichment that is the predominant feature of magma differentiation is in fact paradoxical. The first crystals to precipitate in a multicomponent system are the most refractory, *i.e.*, they have the highest melting points. In accordance with Lindemann's (1910) early ideas, they are assumed to have the strongest interatomic bonds because melting is usually associated with bond breaking caused by mean square vibrational amplitudes exceeding some critical fraction of bond distances. Now, Si–O bonds are commonly supposed to be the strongest in silicate systems because of the small radius (r) and high nominal electrical charge (z) of the Si^{4+} ion compared to those of other major cation-building minerals (Fig. 2). On the basis of ionic forces, one would expect SiO_2 to melt at a much higher temperature than CaO and MgO, but the reverse holds true. Whereas the melting temperature of cristobalite, the high-temperature polymorph of SiO_2 is 1999 K, CaO and MgO melt at temperatures higher than 3000 K. As a consequence, one would expect the silica content to decrease progressively upon fractional crystallization, which clearly contradicts the evolutions that take place along the petrogenetic series.

To account for this anomaly, we will first consider the closely related question of the α–β transitions in tectosilicate minerals, which are accompanied by marked changes in macroscopic properties such as volume (Fig. 3). It is now agreed upon that these transitions represent the

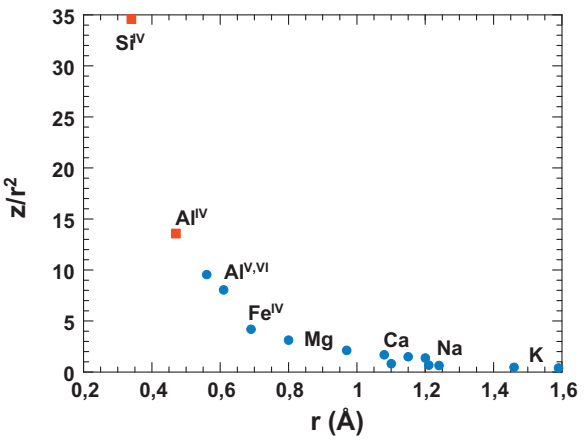

Fig. 2. (Color online.) Decrease with cation radius of the strength of bonds between cations and oxygen as given by variations of field strength, z/r^2. Radii for Si, Al and Fe in the IV- or VI-fold coordination indicated; for alkalis and alkaline earths in coordination states ranging from 6- to 8-fold (radii from Whittaker and Muntus, 1970).

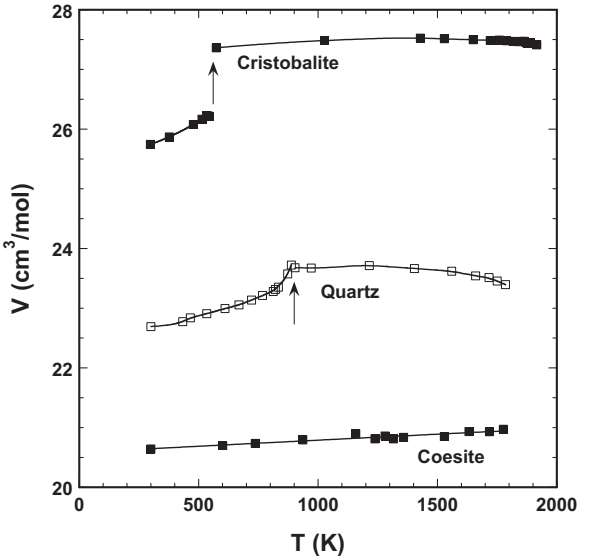

Fig. 3. Effects of α–β transitions (arrows) on the high-temperature volumes of SiO_2 polymorphs. Data of Bourova and Richet (1998) for cristobalite and quartz and Bourova et al. (2006) for coesite.

change from a *static* to a *dynamic* structure when temperature increases. For instance, the Raman-active modes of vibration of cristobalite and carnegieite ($NaAlSiO_4$), which is structurally related to cristobalite, undergo marked modifications at the transition temperatures of 540 and 970 K, respectively (Fig. 4). Then they vary little upon further temperature increases and even upon melting. These modifications are especially clear at low frequencies where the vibrational modes, which involve mainly intertetrahedral motion, merge to form single, broad envelopes similar to those of liquids. Actually, the process at work is free rotation of rigid SiO_4 tetrahedra caused by precession of Si–O–Si linkages with respect to their average orientation (Dove et al., 1997). Interestingly, the entropy changes associated with the α–β transition of these minerals represent more than half and two thirds of the melting reactions of cristobalite and carnegieite, respectively (Table 1). In other words, setting in partial atomic mobility at the α–β transition through motion of oxygen atoms has an entropy cost comparable to disposing of long-range order at the melting point.

Lattice and molecular dynamics simulations have given a more detailed picture of these transitions for SiO_2 polymorphs (Bourova et al., 2000, 2004). The salient point is that, beyond the scale of Si–O tetrahedra, β-cristobalite has a disordered structure at all length scales, which is a dynamical average of three substructures. One of them (α_1) has the same chain arrangement of SiO_4 tetrahedra as α-cristobalite in its tetragonal symmetry (space group $P4_12_12$) with the same value for the intertetrahedral Si–O–Si angle. The two other substructures α_2 and α_3 have different chains of SiO_4 tetrahedra that are derived from α_1 through a 120° rotation around the <111> axis. Because the three substructures have slightly different free energies, the transition from one to the two others is ensured by the thermal energy of oxygen atoms. The motion of a given oxygen atom takes place mainly along

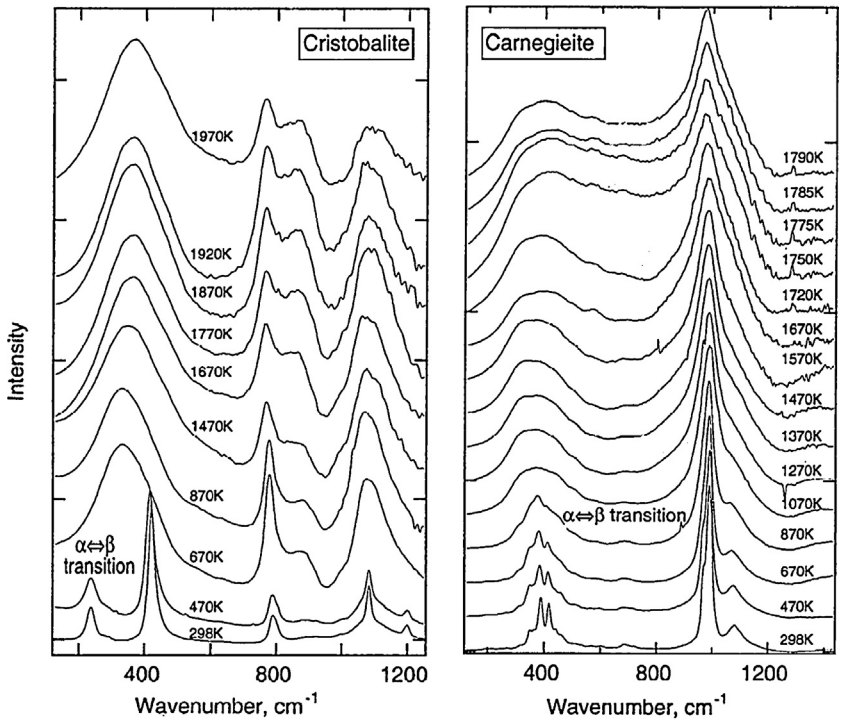

Fig. 4. Contrast between the Raman spectra of cristobalite (SiO_2) and carnegieite ($NaAlSiO_4$) on both sides of the α–β transitions at the temperatures indicated.
Richet and Mysen, 1999.

Table 1
Enthalpy (kJ/mol) and entropy (J/mol K) changes.

Cristobalite Carnegieite		
α–β transition	525 K	965 K
ΔH	1.3	8.1
ΔS	2.5	8.3
Melting	1999 K	1799 K
ΔH	8.9	21.7
ΔS	4.5	12.1

Richet et al., 1982, 1990.

directions perpendicular to other O–O bonds, which correspond to the first O–O distance. Because of the rigidity of the Si–O bond, the vibrational amplitude along these directions is twice larger than in the plane along the Si-Si direction and it keeps increasing with increasing temperature and thermal energy. As for the unit-cell contraction signaled at high-temperatures by the negative thermal expansion coefficient (Fig. 3), it results from the decrease of the first Si-Si distance associated with the large thermal motion of oxygen atoms, which cause the neighboring tetrahedra to come closer to each other.

Although a similar explanation is arrived at for the α–β transition of quartz, an important difference is that the denser arrangement of SiO_4 tetrahedra in quartz compared with cristobalite makes room for only two substructures with similar energies. These are analogous to the Dauphiné twins of α-quartz (α+ and α−), which differ in the orientation of SiO_4 chains around the <001> direction. Turning now to coesite, the densest form of silica with four-fold coordinated Si, we just note that, as experimentally observed (Fig. 3), the monoclinic structure is metastable (with respect to both quartz and SiO_2 liquid) up to the highest temperatures investigated in lattice and molecular dynamics simulations. Thermal expansion is small because a high density limits the extent of rotation of SiO_4 tetrahedra. Above about 1000 K, the structure of coesite nonetheless becomes dynamically disordered and similar to those reported for the β-phases of quartz and cristobalite. Disorder sets smoothly, however, in contrast to its abrupt onset in quartz and cristobalite at their transition temperatures. The radial distribution functions for all bond distances indicate that order then prevails only for the nearest neighbors whereas the angle distributions widen markedly so that the monoclinic form of coesite with a Si–O–Si angle of 180° is just a time-averaged structure. Because all oxygen displacements are strongly anisotropic in both β-quartz and β-cristobalite, disorder in coesite is only partial and affects primarily intrachannel oxygen.

The differences between the three silica polymorphs are sketched in terms of potential energy wells on Fig. 5 with the usual assumption that pressure mostly affects the attractive part of interatomic potentials. Energy minima are thus shifted toward the shorter distances at which strained bonds would match the externally imposed forces. At room temperature the potential of cristobalite has three wells but a single minimum. For quartz, the shift of the energy minima toward higher energies at higher pressure results in the existence of only two wells, which have similar energy minima. At the still higher pressure of formation of coesite, there finally remains a single energy minimum. This sketch has another interesting feature. If one uses Landau's criteria $\delta^2\phi/\delta r^2 = 0$ and $\delta^3\phi/\delta r^3 > 0$ for equilibrium phase transitions (taking the distance r as the relevant order parameter), one sees on Fig. 5 that the temperatures of these transitions decrease from cristobalite to coesite in the order of the reported melting points. For coesite, the melting point would in particular be lower than the temperature of the onset of dynamical disorder and will remain much lower than would be guessed from ionic bonding.

In summary, the anomalously low melting temperature of SiO_2 polymorphs originates in the fact that significant atomic mobility can occur in open three-dimensional networks without requiring Si–O bond breaking. Another manner to view this effect is to invoke the profound contrast between the high rigidity of Si–O bonds and the high flexibility of Si–O–Si angles, which was well illustrated by early quantum-mechanical calculations made for $H_6Si_2O_7$ clusters (Gibbs et al., 1981). As shown on Fig. 6, similar energy variations are caused by 0.02 Å changes of Si–O bond lengths and 20° variations of Si–O–Si angles. As a matter of fact, this result represents a simple justification for the rigid unit model (*e.g.*, Swainson and Dove, 1993) as applied to silicates whereby SiO_4 tetrahedra are taken as rigid units between which tilting results from precession of Si–O bonds around their average orientation. With increasing vibrational amplitudes, the almost constant length of the very strong Si–O bonds then imposes changes in either Si–O–Si angles or Si-Si distances.

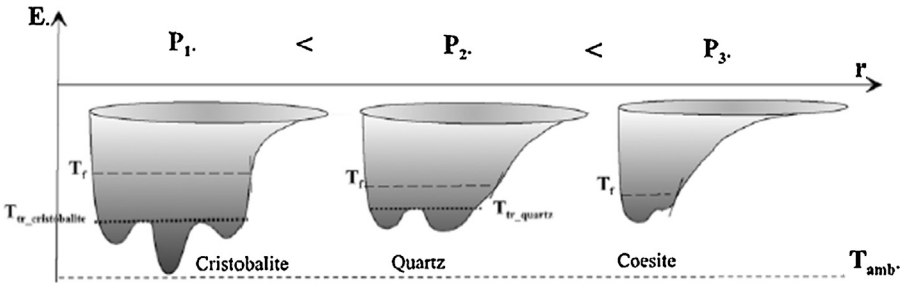

Fig. 5. Potential energy wells of SiO_2 polymorphs against a distance coordinate and their relationships with α–β transitions (T_{tr}) and melting (T_f) temperatures (after Bourova et al., 2006). The dashed lines represent the points where $\delta^2\phi/\delta r^2 = 0$ and $\delta^3\phi/\delta r^3 > 0$.

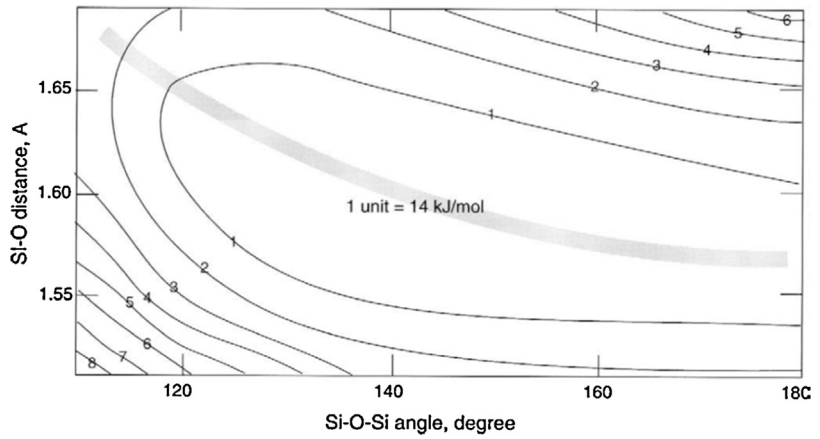

Fig. 6. Contrast between the effects of variations of Si–O distances and Si–O–Si angles on the surfaces of constant energy of $H_6Si_2O_7$ clusters. Gibbs et al., 1981.

3. Orbital hybridization

Of course the directionality of Si–O bonds becomes less important with decreasing SiO_2 content and, thus, with depolymerization of the silicate network so as to vanish for the isolated tetrahedra of the orthosilicate stoichiometry. This strong bond directionality has nonetheless fundamental implications for atomistic simulations of the structure and properties of crystalline or amorphous silicates. For ionic substances, a common starting point in theoretical simulations is for instance the Born–Mayer potential:

$$\phi_{ij}(r_{ij}) = z_i z_j e^2 / r_{ij} + A_{ij} \exp\left(-r_{ij}/\rho_{ij}\right), \quad (1)$$

where the first term represents Coulombic attraction between atoms i and j with formal charges $z_i e$ and $z_j e$ at a distance r_{ij}, whereas the parameter A_{ij} characterizes repulsive forces and ρ_{ij} represents the "softness" of the ion pair. But such a potential is too simple to be adequate for predicting the structure and physical properties of SiO_2-rich phases. To allow for reliable simulations, more complex potentials have been derived from *ab initio* calculations performed on appropriate atomic clusters, which are valuable because they yield truly fundamental insights on the electronic distributions that are actually the main features of interatomic potentials. As derived in this way (Kramer et al., 1991), the potential used for the aforementioned calculations on SiO_2 polymorphs thus for instance accounts well for the strong contrast between the rigidity of Si–O bonds and softness of Si–O–Si linkages (Fig. 6).

Silicon and carbon belong to the same IV-A group of the periodic table. Both have four electrons in their p shell so that their common tetrahedral coordination has long been explained by the formation of four hybrid orbitals sp^3 with either other S or C atoms or with different atoms such as oxygen for Si and hydrogen for C. In silicates, the p shell of silicon is thus filled by outer electrons of the four oxygen donors, which are each directed toward one of the apexes of a regular $[SiO_4]^{4-}$ tetrahedron. The differing principal quantum number n notwithstanding, the analogy between the bond strength-bond energy relationships in the s-p combination for carbon and silicon is almost complete. For both elements, the maximum bond strength (*i.e.*, the angular dependence of the magnitude of a bond orbital) is observed not far from an s:p = 1:3 overall proportion. Although the sp^3 terminology implies that the weights of the respective s and p components of a hybrid sp^3 orbital are indeed in a 1:3 ratio, this condition for bond formation is neither strict nor unique. In addition to the appropriate directionality of the atomic orbitals (AOs), two other conditions have to be satisfied:

- overlapping of discrete AOs on different atoms bonded in the species along the appropriate direction;
- delocalization of electrons between adjacent basins.

Despite the limited basis set of atomic orbitals used in early calculations, correct energies were obtained for molecular orbitals by Collins et al. (1972), who found a considerable participation of the 3d orbital of silicon in the valence orbitals of oxygen to form π-bonding e orbitals and π-bonding t_2 orbitals in the valence region. Interestingly, Collins et al. also noted that the $[SiO_4]^{4-}$ ion cannot exist in the gaseous state because of the presence of 24 electrons in unbound molecular orbitals. Since then the great many *ab initio* calculations performed for Si–O bonding have not changed much the general picture of molecular orbitals in SiO_2. New Density Functional Theory (DFT) calculations for instance confirm former conclusions about the inner orbitals (orbital coefficients and ensuing character assignation, and energy; see Table 2). Rather than reviewing these features, we will just stress two significant points.

The first is the basic role of the medium permittivity. If the $[SiO_4]^{4-}$ group is placed in a reaction field with a permittivity ε of 3.85, which is close to that of molten silica, important changes are observed, at the same theory level, in the orbital populations and energies of both valence and inner regions (Table 2) such that the group becomes "stable" to all extent. If we then perform a Mulliken population analysis on our unstable gaseous ionic cluster

Table 2
Energy and orbital assignments in $[SiO_4]^{4-}$ [a].

Reference	Collins et al. (1972)		This work, in vacuum		This work, $\varepsilon = 3.85$		
Theory level	HF/3-21G(d)		DFT/6-31 + G(d,p)		DFT/6-31 + G(d,p)		
Total energy	−15,632.40		−16,033.53		−16,068.68		
Valence orbitals	$1t_1$	20.54	$3t_1$	18.01	$3t_1$	0.406	
	$5t_2$	18.01	$2e$	16.81			
	$1e$	14.91	$3t_2$	16.68			
	$4t_2$	12.73	$3t_2$	15.04			
	$5a_1$	10.28	$1a_1$	12.76			
			$3t_2$	1.279			
			$1a_1$	0.163			
Mainly O(2s)	$3t_2$	−13.19			Mainly O(2p)	$3t_2$	−0.621
	$4a_1$	−14.15				2e	−0.877
Si(2p)	$2t_2$	−81.59	$3t_2$	−74.41	Si(3p)	$3t_2$	−2.404
Si(2s)	$3a_1$	−134.37	$1a_1$	−119.05	Si(3s)	$1a_1$	−4.526
O(1s)	$2a_1$	−547.12	$1a_1$	−494.67	O(2s,3s)	$3t_2$	−16.306
O(1s)	$1t_2$	−547.12	$3t_2$	−494.67	Si(4s)	$1a_1$	−17.575
Si(1s)	$1a_1$	−1818.63	$1a_1$	−1775.08	Si(2p)	$3t_2$	−91.935
					Si(2s)	$1a_1$	−136.554
					O(1s)	$1a_1$	−512.376
					O(1s)	$3t_2$	−512.376
					Si(1s)	$1a_1$	−1792.530

[a] Density Functional Theory calculations (DFT) carried out with a 6-31 + G(d,p) basis set, *i.e.*, a set of six primitive Gaussians for each core atomic orbital, along with valence orbitals composed of two basis functions each, the first one composed of a linear combination of three primitive Gaussians and the second one consisting of a single primitive Gaussian, with added diffuse (+) and polarization (d,p) components in the framework of DFT with a B3LYP hybrid functional (a mixture of a 3-parameter Hartree–Fock exchange with a Lee–Yan–Parr type exchange correlation).

we obtain a charge of 0.252 *e* localized on the central Si and of −1.063 *e* on each of the four bonded oxygen. But when the ions are placed in the dielectric medium the charge localized on Si increases to 1.917 *e* and that of the four bonded oxygen to −1.479 *e*. As defined by Stewart et al. (1980) in terms of formal and residual charges, the fractional ionic character of the bond is reduced to 0.063 for the isolated cluster (in simple terms, an essentially covalent ionic cluster), whereas $f_i = 0.479$ in the dielectric medium. The permittivity of silica thus has a strong stabilizing effect on $[SiO_4]^{4-}$ groups.

The second point concerns bonding between adjacent $[SiO_4]^{4-}$ groups and the ensuing anomalously low melting temperature of the SiO_2 polymorphs discussed in the previous section. The particular strength of Si–O bonds has the consequence that electron delocalization associated with polymerization through creation of Si–O–Si linkages can be expected neither to be large nor to impose strict geometrical constraints on the arrangements of the $[SiO_4]^{4-}$ building blocks. In other words, the form of MOs eventually encompassing adjacent atomic centers is not *per se* indicative of a bonding condition. The Extended Hückel Molecular Orbital calculations aimed at establishing the extent of bond overlap population *n*(Si–O) and its effect on the cluster geometry carried out by Louisnathan and Gibbs (1972) on both the silicate ion $[SiO_4]^{4-}$ and the orthosilicic acid group $[H_4SiO_4]^{\circ}$ showed a negligible effect of bond overlap on angular distortion. More advanced calculations in terms of electron localization/delocalization through Electron Localization Function or the Laplacian of the electron density (see Gatti, 2005; for an extensive treatment) have been more recently carried out by Gibbs et al. (2003) on geometry optimized $H_6Si_2O_7$ molecule (i.e., for the structure yielded by the minimum of the energy hypersurface) and in coesite to show the extent of bonding and non-bonding regions when one varies the Si–O–Si angle between 110 and 180°.

4. Aluminum charge compensation

Of course, silicon is not the only network-forming cation in silicate crystals and melts. The most important other element to be considered in this respect is aluminum. But for Al^{3+} to substitute for Si^{4+} the deficit of the nominal 3+ charge of Al ions must be compensated, as done in feldspars, by association with either an alkali or half an alkaline earth. When different alkali and alkaline earth cations are present, however, the question arises to determine which ones are the most effective to ensure charge compensation of nominally trivalent aluminum in tetrahedral coordination. To give a firmer theoretical basis to this question *ab initio* calculations have been made on the association with various clusters of SiO_4 and AlO_4 tetrahedra of Na, K, Ca and Mg, the *ad-atoms* (*i.e.*, atoms initially placed at a certain arbitrary distance from the cluster). In a first study (Gatti et al., 2012), we considered 4- to 6-membered rings in which either one or two Al atoms were substituted for Si. Specifically, the energy transfer between the free ion M was investigated in terms of a homogeneous gas-phase reaction of the type:

$$M^{z+} + [Si_{n-m}Al_m(OH_2)_n]^m \rightleftharpoons [MSi_{n-m}Al_m(OH_2)_n]^{(Z-m)} \qquad (2)$$

where Z^+ is the formal charge of the free ion, *m* the number of Al atoms, and *n* that of Si atoms.

The structure of each complex can be determined from the true minimum of the potential energy surface and its energy computed with reference to that of its Al-free counterpart. In this respect, thermal contributions to the thermodynamic functions are negligible compared to the total electronic energy. Barring some stabilizing effects of vibrational motion, the calculated energy changes thus simply reflect electronic energy transfers. For 4-membered rings, the geometry remains largely unaffected by the presence of the ad-atom, the position of the latter within the ring nonetheless depending on its nature (Fig. 7a). More complicated effects are observed in larger rings for which the easily bent Si–O–Si angles allow greater flexibility and, thus, more deformation (Fig. 7b). From a geochemical standpoint, energy calculations have the important consequence that they would make calculations of equilibrium constants possible for the exchange reactions between the various Al-M complexes. Instead of assuming that only one or two M cations act as charge compensators, the actual contribution of each possible cation could then be predicted along with its effects on relevant physical properties.

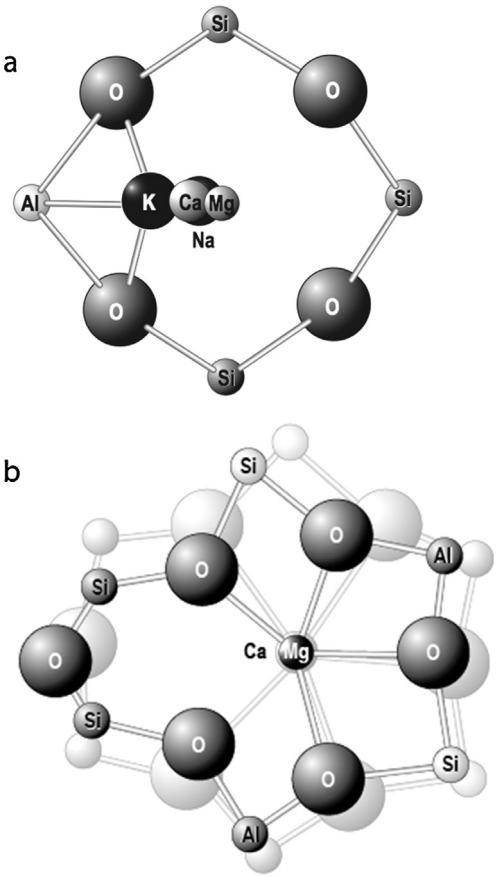

Fig. 7. Planar views of *ab initio* calculated structures: a: monosubstituted four-membered rings along with the various alkali and alkaline earth ad-atoms; b: doubly-substituted six-membered rings with Al in meta positions with alkaline earth ad-atoms. For clarity, the dangling hydrogen bonded to the silicon and aluminum atoms are not shown.

For this purpose, however, it is necessary to perform accurate electron localization/delocalization analyses to determine how the valence electrons redistribute upon alkali or alkaline earth complexation, i.e., how the electrons of the various molecular orbitals redistribute among the adjacent basins of the ring network (Gatti et al., 2012). As found earlier for crystal-like aluminosilicate complexes (Vayssilov et al., 2000), one observes that the stabilization of O1*s* orbitals in the Si–Al cluster exceeds by far the amount of electronic energy gained in complexation, which indicates that a substantial redistribution is operating throughout the complex. The Al-free 4-membered ring may be interpreted as stabilizing a Pauling double bond because it has a low-lying molecular orbital essentially constituted of the *s* orbitals of oxygen with some contribution from *s* orbitals of silicon. In a 3-d representation, the electron cloud of this σ-bonding molecular orbital appears delocalized on the four oxygen donor centers on the *xy* plane of the ring when arranged in a standard configuration.

In 6-membered Al-free rings an orbital of nearly identical energy is observed. This orbital is essentially composed of the s AO of all oxygen donor centers, with minor contributions from the Si atoms. The substitution of one or two Si atoms of the ring with Al has some perturbation effect on the density distribution. Whereas in the case of the silico-aluminate 4-membered ring the apparent delocalization still operates on all donor centers, in the monosubstituted 6-membered ring the delocalization excludes the two donor centers nearest to Al. The Pauling double bond is apparently present in linear chains as well, such as the $[Si_2O_7]^{6-}$ dimers. Also in this case all oxygen centers in the cluster are surrounded by the electron cloud, which excludes the central metals (*i.e.*, not only the bridging oxygen but also the singly bonded ones). Further calculations are required to check this point for clusters with different geometries. But the facts that the same Al-compensation mechanism seems to operate over the whole geochemically range of melt composition, and to affect linear chains as well, suggest that the effect is fairly general.

5. Noble gas solubility

When dealing with volatile solubility, electrostatic, dispersive (van der Waals) and repulsive solute-solvent interactions must be taken into account. All three are quantum-mechanical in origin and may be addressed theoretically with the appropriate choice of functional theory level and basis set. In addition, a fourth factor must be considered, namely, the cavitation energy of the solute, *i.e.*, the energy needed to form cavities in the solvent appropriate for hosting solute species. In physical chemistry these contributions are so well known that solvent properties (molecular radius, dielectric constant, etc.) are conformed to the observed solubility of some noble gas (*e.g.*, He in water or benzene) in the most widely used quantum-mechanical computational packages.

In geochemistry, however, one generally assumes that species such as noble gases do not interact with the aqueous or silicate species among which they are hosted in

the available cavities of the solution (*e.g.*, Bouhifd et al., 2008; Chamorro-Perez et al., 1998). This assumption is actually too simple so that it prevents the solubility of these "inert" gases in aqueous and silicate solutions from being understood at a fundamental level. Actually, the bulk Gibbs free energy of solution for a gaseous species in its stable standard state is simply related to the Henry's Law constant K_H by:

$$\Delta G_S = RT\ln K_H = \Delta\bar{G}_{cav} + \Delta\bar{G}_{el} + \Delta\bar{G}_{disp} + \Delta\bar{G}_{rep} + RT\ln\left(\frac{RT}{\bar{V}_s}\right) \quad (3)$$

where R is the gas constant, T the temperature, $\bar{V}_s$ the molar volume of the solvent and where the ΔG terms refer to the cavitation, electrostatic, dispersive and repulsive contributions. Within the framework of the quantum Polarized Continuum Model, one can evaluate the relative importance of these contributions by including cavitation effects with a quasi-classical approach. Such calculations have been made for a variety of silicate melts for which the solubility of noble gases is known (Ottonello and Richet, 2014). Typical results for the various ΔG terms of eq. (3) are shown on Fig. 8 for one mole of dissolved gas at 1 bar, 25 °C in a medium that simulates a tholeiite melt (i.e., static dielectric constant $\varepsilon = 5.125$, solvation radius $\sigma_s/2 = 1.526$ Å, number density = 0.02508 Å^{-3}). In agreement with the fact that noble gases have a spherical shape and weakly interact electronically with the solvent, the repulsive and especially the electrostatic contributions to ΔG_s are negligible. But the commonly assumed inert nature of noble gases is not borne out because dispersive effects are in contrast significant, with an influence that increases with increasing polarizability (and atomic radius) of the noble gas.

Although quantum-mechanical dispersion effects thus have to be addressed, the main factor in eq. (3) is the cavitation energy on which we will thus focus here. The diameter of the solvent is a thermally averaged quantity over various orientations of the solvent with respect to the cavity surface. If we denote it by σ_s, the problem is to evaluate the reversible work W_0 necessary to create in the solvent a cavity of radius $r \le \sigma_s/2$. To solve this problem,

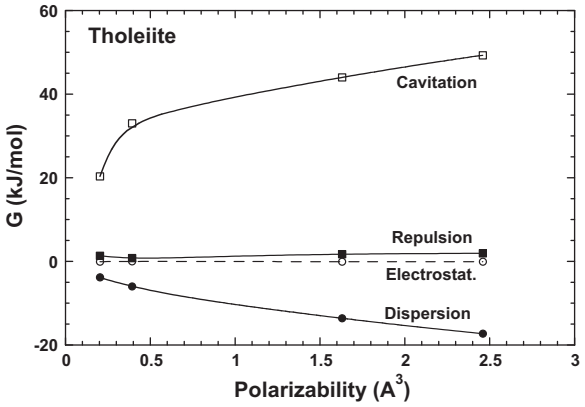

Fig. 8. Contributions to the Gibbs free energy of solvation at 25 °C in a tholeiite-like medium against the polarizability of noble gases.

we used the formulation based on the scaled particle theory (SPT) of Reiss and coworkers (Reiss et al., 1960) with which Pierotti (1976) obtained:

$$W_0(r,\rho) = kT\ln p_{0,i}, \quad (4)$$

where k is the Boltzmann constant. As to $p_{0,i}$, the complement to 1 of the probability of finding a solute molecule i at the place of a solvent molecular center, Pierotti (1976) then obtained:

$$p_{0,i} = (1 - p_{0,r}) = \left(1 - \frac{4}{3}\pi r^3\rho_s\right). \quad (5)$$

To make room in the solvent for a solute of diameter σ_i the necessary cavity must have a radius $r = \frac{\sigma_s+\sigma_i}{2}$. Denoting by $Y = \frac{\pi\rho_s\sigma_s}{6}$ the reduced number density and by $\varsigma = \sigma_i/\sigma_s$, Pierotti (1976) rewrote the work as:

$$\frac{W(r,\rho)}{kT} = -\ln(1-Y) + \left(\frac{3Y}{1-Y}\right)\varsigma + \left[\left(\frac{3Y}{1-Y}\right) + \frac{9}{2}\left(\frac{Y}{1-Y}\right)^2\right]\varsigma^2 + \frac{YP}{\rho_s kT}\varsigma^3 \quad (6)$$

where P is the (hydrostatic) pressure. The partial molar Gibbs free energy of cavitation may then be assumed to be equal to the reversible work $\bar{G}_{cav} = W(r,\rho) \equiv \Delta G_{cav}$. As a result, the cavitation enthalpy has the following form:

$$H_{cav} = Y\alpha_V RT^2(1-Y)^{-3}\left[(1-Y)^2 + 3(1-Y)\varsigma + 3(1+2Y)\varsigma^2\right] + \frac{N_0 P}{\rho}\varsigma^3 \quad (7)$$

whereas the cavitation entropy may be obtained from the thermodynamic relationship $S_{cav} = (\Delta G_{cav} - H_{cav})/T$ (Pierotti, 1976).

With this formalism, one finds that the solvent radius σ_s is satisfactorily reproduced by a simple expression of the form $\sigma_S = 2 \times (1.1383 r_{coll} - 0.3836)$ where r_{coll} is the collisional radius (*i.e.*, $r_{coll} = \sqrt[3]{V}/8$; Stearn and Eyring, 1937). The striking feature is that this expression fits nicely the observed solubility trends for noble gases in a variety of solvents that include non-polar (C_6H_6) and polar (H_2O) liquids. The major feature of this rather simple formalism thus is that a volatile species does not dissolve in pre-existing cavities, but in cavities that are formed by interaction with the solute. Assessment of noble gas solubility in various fluids then is a simple but stringent test of the reliability of the parameterization adopted to model the Gibbs free energy of cavitation. Based on the wealth of solubility experiments carried out by geochemists through the decades, it is possible to retrieve not only the thermodynamic parameters of the various solutes, but also the solvent properties needed to determine the solubilities observed at high-temperatures and pressures through inverse methods (Ottonello and Richet, 2014).

6. Conclusions

Since the physical and chemical properties of macroscopic bodies are determined from those of their atomic constituents, fundamental insights on these properties have to be derived from accurate descriptions of bonding at

an atomic level. To illustrate the kind of work to be done to understand the Earth's structure and dynamics at a really fundamental level, this review has dealt with a few important topics but is clearly not comprehensive; volatile dissolution or phase diagram calculations are just two examples among the great many other features that can be investigated. In this respect, it is well known that, over experiments, calculations have the great advantage of being performed as readily under extreme conditions as under room pressure and temperature. The composition ranges studied can also be varied at will to address the very large diversity of natural conditions. Even though the size of the system that can be investigated is still limited in terms of number of atoms and, thus of structural complexity, continuous improvements in computer power will continue to alleviate this problem.

Acknowledgments

We thank E. Bourova, C. Gatti, B.O. Mysen and M. Vetuschi Zuccholini for fruitful collaboration on these topics, and J. Badro and V. Courtillot for comments. G.O. also thanks IPGP for visiting positions during which he contributed to this work.

References

Bouhifd, A., Jephcoat, A.P., Kelley, S.P., 2008. Argon solubility drop in silicate melts at high pressures: a review of recent experiments. Chem. Geol. 256, 252–258.

Bourova, E., Richet, P., 1998. Quartz and cristobalite: high-temperature cell parameters and volume of melting. Geophys. Res. Lett. 25, 2333–2336.

Bourova, E., Parker, S.C., Richet, P., 2000. Atomistic simulations of cristobalite at high-temperatures. Phys. Rev. B: Condens. Matter 62, 12052–12061.

Bourova, E., Parker, S.C., Richet, P., 2004. High-temperature structure and dynamics of coesite (SiO_2) from numerical simulations. Phys. Chem. Miner. 31 (2004), 569–579.

Bourova, E., Richet, P., Petitet, J.-P., 2006. Coesite (SiO_2) as an extreme case of superheated crystal: an X-ray diffraction study up to 1776 K. Chem. Geol. 229, 57–63.

Chamorro-Perez, E.M., Gillet, P., Jambon, A., Badro, J., McMillan, P., 1998. Low argon solubility in silicate melts at high pressure. Nature 393, 352–355.

Collins, G.A.D., Cruikshank, D.W.J., Breeze, A., 1972. *Ab initio* calculations of the silicate ion, orthosilicic and their L2,3 X-ray spectra. J. Chem. Soc. Faraday Trans. II 68, 1189–1905.

Cox, K.G., Bell, J.D., Pankhurst, R.J., 1979. The Interpretation of Igneous Rocks. George Allen and Unwin, London.

Dove, M.T., Keen, D.A., Hannon, A.C., Swainson, I.P., 1997. Direct measurements of the Si–O bond length and orientational disorder in the high-temperature phase of cristobalite. Phys. Chem. Miner. 24, 311–317.

Gatti, C., 2005. Chemical bonding in crystals: new directions. Z. Kristall. 220, 299–457.

Gatti, C., Ottonello, G., Richet, P., 2012. Energetics and donor-acceptor relations in aluminosilicate rings with alkali and alkaline earth charge-compensating cations. J. Phys. Chem. A 116, 8584–8598.

Gibbs, G.V., Meagher, E.P., Newton, M.D., Swanson, D.K., 1981. A comparison of experimental and theoretical bond length and angle variations for minerals and inorganic solids, and molecules. In: O'Keefe, M., Navrotsky, A. (Eds.), Structure and Bonding in Crystals, Vol. I, Academic Press, New York, pp. 195–225.

Gibbs, G.V., Cox, D.F., Boisen Jr., M.B., Down, R.T., Ross, N.L., 2003. The electron localization function: a tool for locating favorable proton docking sites in the silica polymorphs. Phys. Chem. Miner. 30, 305–316.

Ispas, S., Benoît, M., Jund, P., Julien, R., 2001. Structural and electronic properties of the sodium disilicate glass $Na_2Si_4O_9$ from classical and *ab initio* molecular dynamics simulations. Phys. Rev. B: Condens. Matter 64, 214206–214211.

Kramer, G.J., Farrgher, N.P., van Beest, B.W.H., 1991. Interaction force fields for silicas, aluminosphosphates, and zeolites: derivation based on *ab initio* calculations. Phys. Rev. B: Condens. Matter 43, 5068–5080.

Lindemann, F.A., 1910. Über die Berchnung molekulaner Eigenfrequenzen. Phys. Z. 11, 609–612.

Louisnathan, S.J., Gibbs, G.V., 1972. The effect of tetrahedral angles on Si–O bond overlap populations for isolated tetrahedra. Am. Miner. 57, 1614–1642.

Mysen, B.O., Richet, P., 2005. Silicate Glasses and Melts. Properties and Structure. Elsevier, Amsterdam.

Osborn, E.F., 1950. Segregation of elements during the crystallization of a magma. J. Am. Ceram. Soc. 33, 219–224.

Ottonello, G., Richet, P., 2014. The solvation radius of silicate melts based on the solubility of noble gases and scaled particle theory. J. Chem. Phys. 140, 044506.

Ozima, M., Pososek, F.A., 2001. Noble Gas Geochemistry. Cambridge University Press, Cambridge, UK.

Pierotti, R.A., 1976. A scaled particle theory of aqueous and nonaqueous solutions. Chem. Rev. 76, 717–726.

Reiss, H., Frisch, H.L., Helfand, E., Lebowitz, J.L., 1960. Aspects of the statistical thermodynamics of real fluids. J. Chem. Phys. 32, 119–124.

Richet, P., Bottinga, Y., Deniélou, L., Petitet, J.-P., Téqui, C., 1982. Thermodynamic properties of quartz, cristobalite and amorphous SiO_2: drop calorimetry measurements between 1000 and 1800 K and a review from 0 to 2000 K. Geochim. Cosmochim. Acta 46, 2639–2658.

Richet, P., Robie, R.A., Rogez, J., Hemingway, B.S., Courtial, P., Téqui, C., 1990. Thermodynamics of open networks: ordering and entropy in $NaAlSiO_4$ glass, liquid and polymorphs. Phys. Chem. Miner. 17, 385–394.

Richet, P., Mysen, B.O., 1999. High-temperature dynamics from Raman spectroscopy in cristobalite (SiO_2) and carnegieite ($NaAlSiO_4$). Geophys. Res. Lett. 26, 2286.

Stearn, A.E., Eyring, H., 1937. The deduction of reaction mechanisms from the theory of absolute rates. J. Chem. Phys. 5, 113–124.

Stewart, R.F., Whitehead, M.A., Donnay, G., 1980. The ionicity of the Si–O bond in low-quartz. Am. Miner. 65, 324–326.

Swainson, I.P., Dove, M., 1993. Low-frequency floppy modes in β-cristobalite. Phys. Rev. Lett. 71, 193–196.

Tossel, J.A., Vaughan, D.J., 1992. Theoretical Geochemistry: Application of Quantum Mechanics in the Earth and Mineral Sciences. Oxford University Press, Oxford, UK.

Vayssilov, G.N., Lercher, J.A., Rösch, N.J., 2000. Interaction of methanol with alkali metal exchanged molecular sieves. 2. Density functional study. J. Phys. Chem. B 104, 8614–8623.

Whittaker, E.J.W., Muntus, R., 1970. Ionic radii for use in geochemistry. Geochim. Cosmochim. Acta 34, 945–957.